Journal of Visual Communication and Image Representation 50 (2018) 9–15

Contents lists available at ScienceDirect

Journal of Visual Communication and Image Representation

journal homepage: www.elsevier.com/locate/jvci

Color image dehazing using surround filter and dark channel prior☆

Deepa Nair*, Praveen Sankaran

Electronics and Communication Engineering Department, National Institute of Technology Calicut, 673601, India

ARTICLE INFO

Keywords:
Atmospheric light
Color space
Dark channel prior
Dehazing
No reference quality assessment
Transmission map

ABSTRACT

Outdoor images are often degraded by haze, resulting in a distinctive gray or bluish hue which diminishes visibility. Of the existing haze removal methods, the ones that are effective are computationally complex and memory intensive. In this paper, we propose a simple haze removal technique, whose computational complexity is that of a simple convolution. To this purpose, a center surround filter is employed to improve speed and memory requirements of the transmission estimation in image dehazing. This can be useful for real time applications such as driver assistance, runway hazard detection and surveillance. The proposed technique relies on deriving an alternative transmission estimate by filtering the input image in three different color spaces, namely RGB, Lab and HSV. The effectiveness of the proposed method is compared with that of other state of the art methods using a subjective quality assessment method and a number of objective quality assessment methods.

1. Introduction

Haze is an atmospheric effect which forms a gray or bluish hue over the scene, thus diminishing visibility in outdoor images. Particles such as smoke, moisture, dust and vapor present in the atmosphere scatter light and cause the formation of haze [1]. The manner in which a particle scatters incident light depends on the material properties, shape and size of the former. The process of removing haze effects from outdoor images and recovering the true color details is called dehazing. This can improve visibility, make images more pleasing and can be employed for applications such as runway hazard detection, target recognition and driver assistance. Our main contributions are overcoming the memory issues while processing large images and speeding up the dehazing process.

Koschmieder's mathematical model represented by Eq. (1) is widely used for expressing the image formation model mathematically [2].

$$E(x,y) = t(x,y) \times E_o(x,y) + (1-t(x,y)) \times A, \quad (1)$$

where $E(x,y)$ is the observed intensity of the pixel of the hazy image at position (x,y), $E_o(x,y)$ is the corresponding pixel intensity of the haze free image to be obtained, $t(x,y)$ is the medium transmission which is the part of the light that is not scattered and reaches the observer and A is the global atmospheric light representing the scattering of light by the atmospheric particles [3]. The term $t(x,y) \times E_o(x,y)$ describes the direct transmission. It is a multiplicative distortion of the scene radiance. The term $(1-t(x,y))A$ results from scattered light and is an additive component which leads to the shift of scene colors [1,4]. When the atmosphere is homogeneous, the transmission t can be expressed as,

$$t(x,y) = e^{-\beta d(x,y)}, \quad (2)$$

where β is the scattering coefficient of the atmosphere and d is the scene depth. This equation indicates that the scene radiance is attenuated exponentially with the depth. If the values of $t$and $A$are known, the dehazed image E_0 can be obtained from Eq. (1).

In the next section, the background of this proposal is discussed. Section 3 describes the proposed method in three color spaces and the fusion method used as post processing for visual enhancement. In Section 4, different quality assessment strategies are explained. This is followed by analysis of the results and the conclusion.

2. Background

There are many single image dehazing methods available in the literature. One such popular method is based on the dark channel prior (DCP). He et al. [3] describe the concept of the dark channel based on the observation that "in a clear day image, except for the sky regions, the intensity of each pixel will be close to zero at least in one color channel". This statistical observation is called dark channel prior.

The additive atmospheric light in the hazy image makes it brighter than its haze free version. So, the dark channel of a hazy image will have higher intensity than its haze free version. Also, intensity will be higher in regions with denser haze. So the thickness of haze can be

☆ This paper has been recommended for acceptance by Zicheng Liu.

* Corresponding author.
E-mail address: psankaran@nitc.ac.in (P. Sankaran).
URL: http://www.nitc.ac.in (P. Sankaran).

https://doi.org/10.1016/j.jvcir.2017.11.005
Received 23 January 2017; Received in revised form 14 May 2017; Accepted 5 November 2017
Available online 06 November 2017
1047-3203/

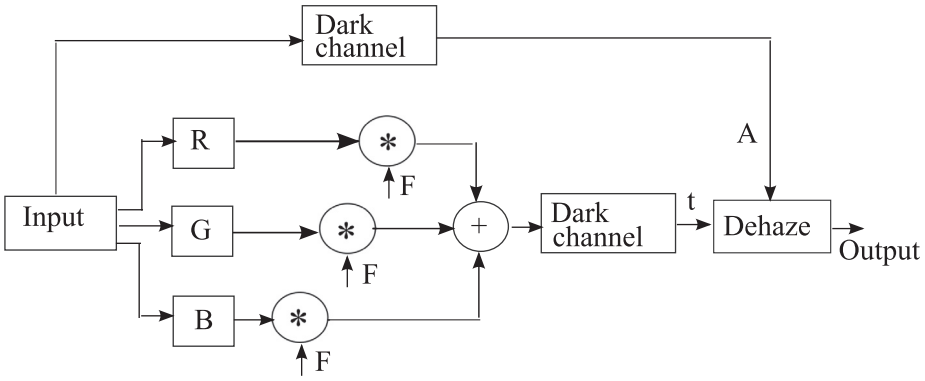

Fig. 1. Surround filter applied on RGB channels.

roughly represented by the intensity of the dark channel, which is used to estimate atmospheric light and the transmission map. The transmission map estimated using dark channel prior requires refinement to avoid halo and blocking artifacts. The Laplacian matrix used for refinement makes this method complex and time consuming [3]. Employing a guided image filter for the refinement reduces the complexity [5]. Other effective dehazing methods are proposed by Fattal [6], Tarel [7] and Qi et al. [8]. In Fattal's method, the output depends largely on the quality of the input. Tarel's method, though implemented through simple steps, assumes some parameters. Yu et al. directly calculate the transmission map by interpolating the minimum channel image and the block wise dark channel by controlling the weight by a Gaussian function [9]. A guided joint bilateral filter is used by Xiao et al. to obtain the refined transmission map [10].

Knowing the close relationship between the color constancy of human visual system and retinex [11], which makes use of a Gaussian surround filter, we explore the possibilities of using a surround filter in different color spaces for dehazing natural outdoor images.

In this paper, we propose a method that makes use of a center/surround filter for single image dehazing. Our method is based on the haze image model represented by Eq. (1). To solve this model and get the clear image, the transmission map and the atmospheric light are to be calculated. For this, we employ a surround filter and the theory of the dark channel prior to formulate a simple method to obtain the transmission map. Then the haze image model is solved in three different color spaces and the results are compared with that of eight other methods provided by IVCDehazedataset [12,13].

3. The proposed method

Haze is modeled as an additive component by Koschmieder. To solve this model and retrieve the clear image, the transmission map t needs to be calculated. Haze is assumed to be the corrupting effect of illumination. It is known that illumination component of an image is slowly varying. For an image which is not corrupted with illumination component, the low frequency components will be small. So a low pass filter is used as the first step to obtain the transmission map. Though low pass filtering can be done in different ways, the Gaussian function is preferred because it results in lightness and color rendition [14]. Also the Gaussian function is proved to be useful in removing the discontinuities [15]. So using the Gaussian filter for obtaining the transmission map would automatically provide a smoothing effect.

In this paper, we dehaze the input image in three different color spaces and compare their quality with other proven methods. First the dehazing process is performed in RGB space considering each color channel separately. Then dehazing is performed in HSV and Lab color spaces. Lab color space is capable of reflecting the perception characteristics of the human visual system well [16]. HSV and Lab color spaces separate color from intensity, unlike RGB color space [17]. So in HSV and Lab color spaces, only the intensity component is processed for the calculation of the transmission map, while the color components are maintained to reduce color distortion [18].

3.1. Atmospheric light estimation

In all the three proposed cases, the atmospheric light is estimated using the dark channel of the image, which is the result of two minimum operations. To calculate the dark channel of the image, the minimum intensity of each pixel considering all the three color channels is calculated. Then this minimum image is divided into patches. All the pixels in each patch are replaced by the minimum intensity in the corresponding patch to get the dark channel of the image. 0.1% of the brightest n pixels in the dark channel are selected. The average of the pixel intensities in the original image corresponding to these selected pixels is the atmospheric light A.

3.2. Surround filter in RGB

The filtering operation using the Gaussian function is performed on each color band as shown in Eq. (3).

$$E^b_{LP}(x,y) = F(x,y) * E^b(x,y) \tag{3}$$

F is the Gaussian surround filter given by,

$$F(x,y) = Ke^{-\sqrt{x^2+y^2}/c^2}, \tag{4}$$

where (x,y) represents a pixel location and c is the surround constant. K is assumed to be 1. E is the hazy image and b represents the color band. The results in three color bands are concatenated to get a three channel image E_{LP}. The dark channel of this image is calculated as . The resulting values are scaled and the final transmission map $t(x,y)$ is obtained as per Eq. (5).

$$t(x,y) = 1 - \tilde{t}(x,y) \tag{5}$$

The atmospheric light is calculated as described in Section 3.1 and dehazing is performed using Eq. (1). The block diagram in Fig. 1 describes this method. It is found that for different hazy images, optimum output is obtained for different values of the surround constant c. So the selection of the value of c is very critical for this application. Appropriate values of c are selected for each color channel to get the best results. It is found that for obtaining appealing results, the values of c that should be selected vary from 15 to 250. Three different values, one low, one medium and the third large give appealing results for most of the input images.

3.3. Surround filter in HSV

Here, the image is converted into HSV color space and the value component V alone is convolved with Gaussian filter.

$$\tilde{t}(x,y) = F(x,y) * V(x,y), \tag{6}$$

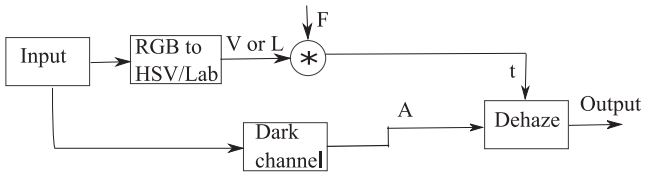

Fig. 2. Dehazing using surround filter on intensity component.

where F is the Gaussian surround filter given by Eq. (4). The final transmission map $t(x,y)$ is obtained as per Eq. (5).

Once the atmospheric light and the transmission map are available, the clear image can be obtained from Eq. (1). The block diagram representation of this method is shown in Fig. 2. In this case, only the Vcomponent is processed.

3.4. Surround filter in Lab

The image is converted into Lab color space and the lightness component L alone is convolved with Gaussian filter. The transmission map is calculated as described in Section 3.3 and the atmospheric light as per Section 3.1. The block diagram representation is the same as Fig. 2 with L as the input to the convolution block.

Our method for calculating the transmission map involves convolution operation between a two dimensional image and a two dimensional filter. The computational complexity of this can be represented as $\mathcal{O}(MNmn)$, where MN is the size of the two dimensional image and mn is the size of the filter, both represented in terms of number of pixels. No separate refinement method for smoothing the transmission map is used. This makes our method simple and fast. A parallel framework on many-core processors can speed up our method further compared to serial execution [19,20].

Our method applied to a large image of size 3103×5516 results in images shown in Fig. 4. Conventional methods with Laplacian matting will not work on such large images because of memory constraints. Haze is completely removed from the near as well as the distant parts of the image. But it results in a dark image with unnatural colors in some parts of the image. To improve the visual appeal of the dehazed image, we use a fusion method as post processing which is described in the next section.

3.5. Image fusion for visual appeal

Introducing a small amount of haze improves the naturalness of the dehazed image which is very dark. So it is fused with the original hazy image using wavelet fusion [21]. This involves Laplacian decomposition of the images and a Gaussian pyramid of the weight maps. Colorless regions are given less weight, while interesting areas containing bright colors and details are preserved.

An indicator C for contrast is calculated by applying a Laplacian filter to the gray scale version of the image, and taking the absolute value of the filter response. It tends to assign a high weight to important elements such as edges and texture. A saturation measure S is computed as the standard deviation within the R, G and B channel, at each pixel. Since intensities near zero (underexposed) or one (overexposed) are undesirable, each intensity is weighted based on how close it is to 0.5 using a Gauss curve $\exp\left(\frac{-(i-0.5)^2}{2\sigma^2}\right)$, where σ is taken as 0.2. To account for multiple color channels, the Gauss curve is applied to each channel separately, and the results are multiplied to get the measure of exposedness E. For each pixel, the information from the different measures are combined into a scalar weight map using multiplication. The fused image is obtained from these Laplacian pyramids and the Gaussian weight maps as shown in Fig. 3.

Fig. 4 shows the result of the fusion operation on the input image and the output considering V. The result of the fusion using the input image and the output considering L is shown in Fig. 5. The dehazed image before applying fusion and the respective histograms are also shown for comparison. The resulting post processed image has a histogram with a better spread than that of the dehazed image. A well spread histogram indicates an image with good contrast. Since fusion step adds some amount of haze to the result, this step need be performed only if the dehazed image is very dark as in the case of a large image. This step is not performed on the results obtained using IVC-Dehazedataset.

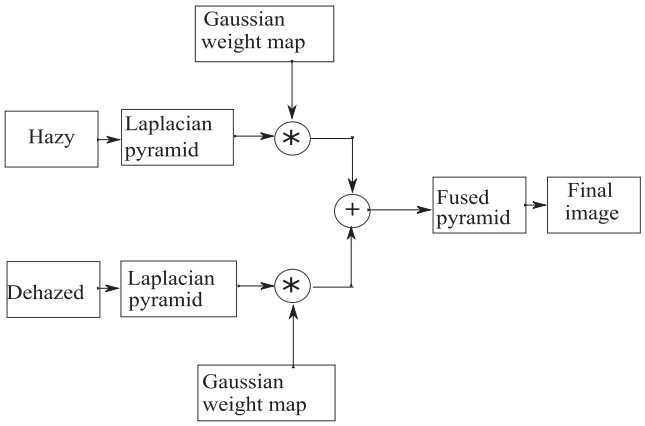

Fig. 3. Block diagram of fusion as post processing.

4. Image quality assessment

"Image quality assessment (IQA) methods enable us to quantify the visual quality of an image in a manner that agrees with human subjective rating" [22]. IQA methods can generally be categorized into two - subjective methods and objective methods. It is not possible to integrate subjective image quality assessment methods into real-time automatic systems. In such cases, objective methods have to be used. Based on the availability of distortion-free original image, objective quality assessment techniques can further be classified into three, namely full reference (FR), reduced reference (RR) and no reference (NR) techniques [23,24]. Haze effects cannot be addressed like classical image noise or degradation which might be added and then removed. Moreover, in the case of dehazing of a natural image, the reference or clear image is not available. So to analyse our result images, blind enhancement assessment method is used [25,26]. Haze removal is performed on hazy images of different sizes varying from 512×300 to 512×384 pixels using different methods. The evaluation descriptors calculated are shown in Table 1.

4.1. Subjective IQA

A visual comparison between the results was performed for obtaining the mean opinion score (MOS). Total 25 hazy images were used. One hazy source image is dehazed in three different color spaces using our method. Considering six more other methods, there are total ten dehazed images corresponding to each input hazy image. Twenty annotators were asked to rate each of the ten images on a scale 0–10. The absence of haze, the naturalness of colors and details present in the image are the criteria based on which the annotators were asked to rate the images. The annotators were not told which result is for which dehazing method. The display screen was set at a resolution of 1920×1080 pixels and the test images were displayed with black background on 21.5″ LCD monitor (Dell E2214H). The annotators viewed the monitor approximately from a distance of twice the screen height. From the ratings by the annotators, the MOS is calculated for each of the ten dehazed images.

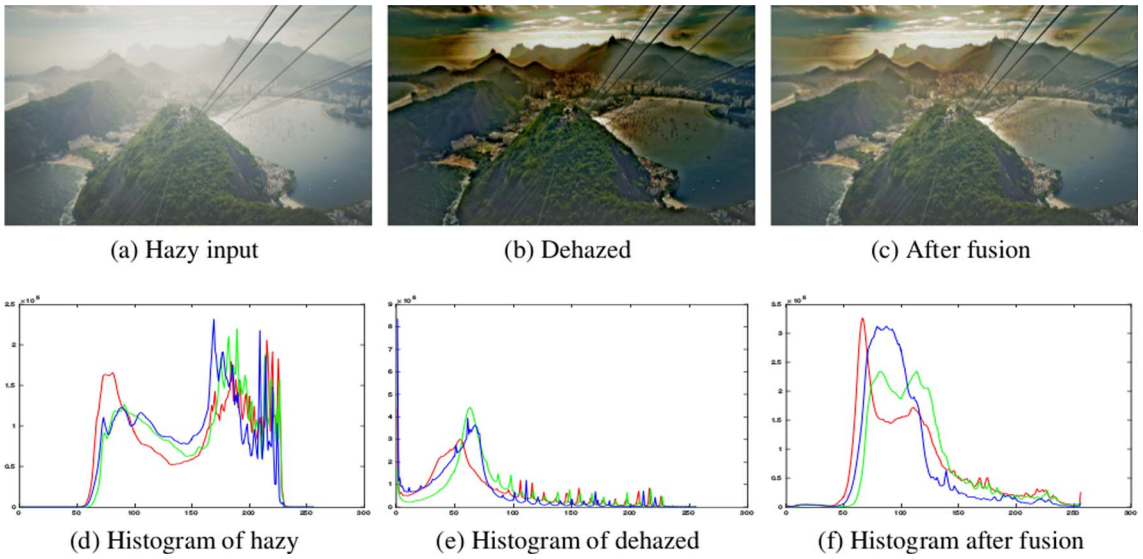

Fig. 4. Fusion applied to dehazing on HSV and the corresponding histogram.

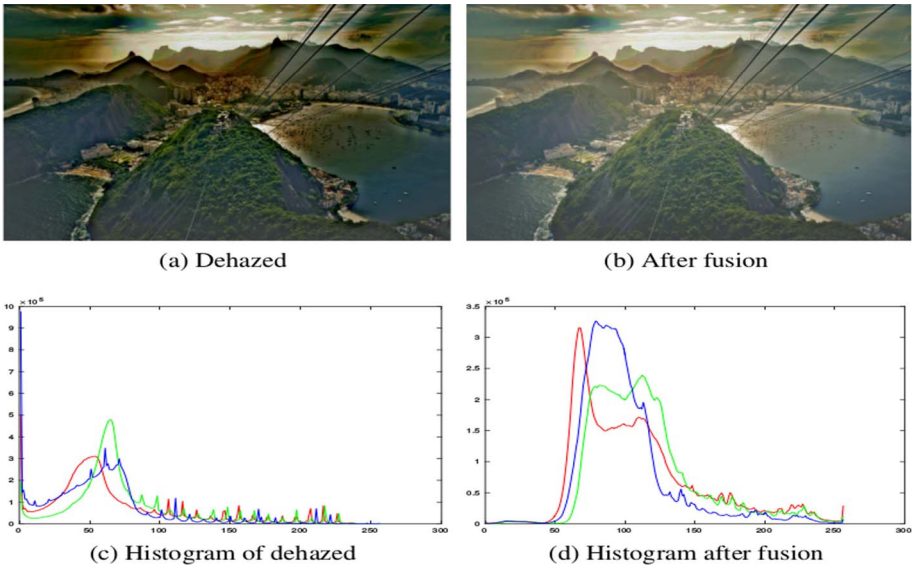

Fig. 5. Fusion applied to dehazing on Lab and the corresponding histogram.

4.2. Full reference IQA

To compare different dehazing methods, full reference IQA methods like Structural similarity (SSIM) [27] and Visual information fidelity criterion (VIF) can be used. Information fidelity methods exploit the relationship between statistical image information and visual quality [28,29]. Visual information fidelity (VIF) is the visual quality of the degraded test image computed as the amount of mutual information shared between the test and the reference images. As image dehazing has enhancement effect on the image, VIF in reverse mode (VIF(R)) is

Table 1
Quantitative evaluation of different dehazing methods.

IQA →	No reference					Full reference	Subjective
Dehazing ↓	e	σ	$\bar{r}$	D	SD	VIF(R)	MOS
He09	1.0097	0.0029	1.5748	1.5578	50.7354	0.7640	5.4175
Kim13	0.7497	0.0537	2.2789	0.5363	61.7729	0.5711	6.3600
Kolor	0.5870	0.0152	1.4649	0.4649	52.3532	0.7580	6.6100
Meng13	1.1844	0.0027	2.2510	0.4446	54.6409	0.5908	5.7800
Tang14	0.9928	0.0018	1.6482	0.5853	50.3956	0.7411	5.8075
Tarel09	2.7571	0.0000	3.7969	0.5115	61.8466	0.4663	4.1493
Xiao12	2.7571	0.0000	3.7969	0.5002	61.8466	0.6319	6.2308
HSV	1.1898	0.0000	1.9104	0.5243	72.3524	0.3997	4.9233
Lab	1.1409	0.0000	1.9676	0.5208	61.6829	0.5126	4.9480
RGB	1.2527	0.0000	2.9689	0.2706	69.1186	0.4695	5.7360

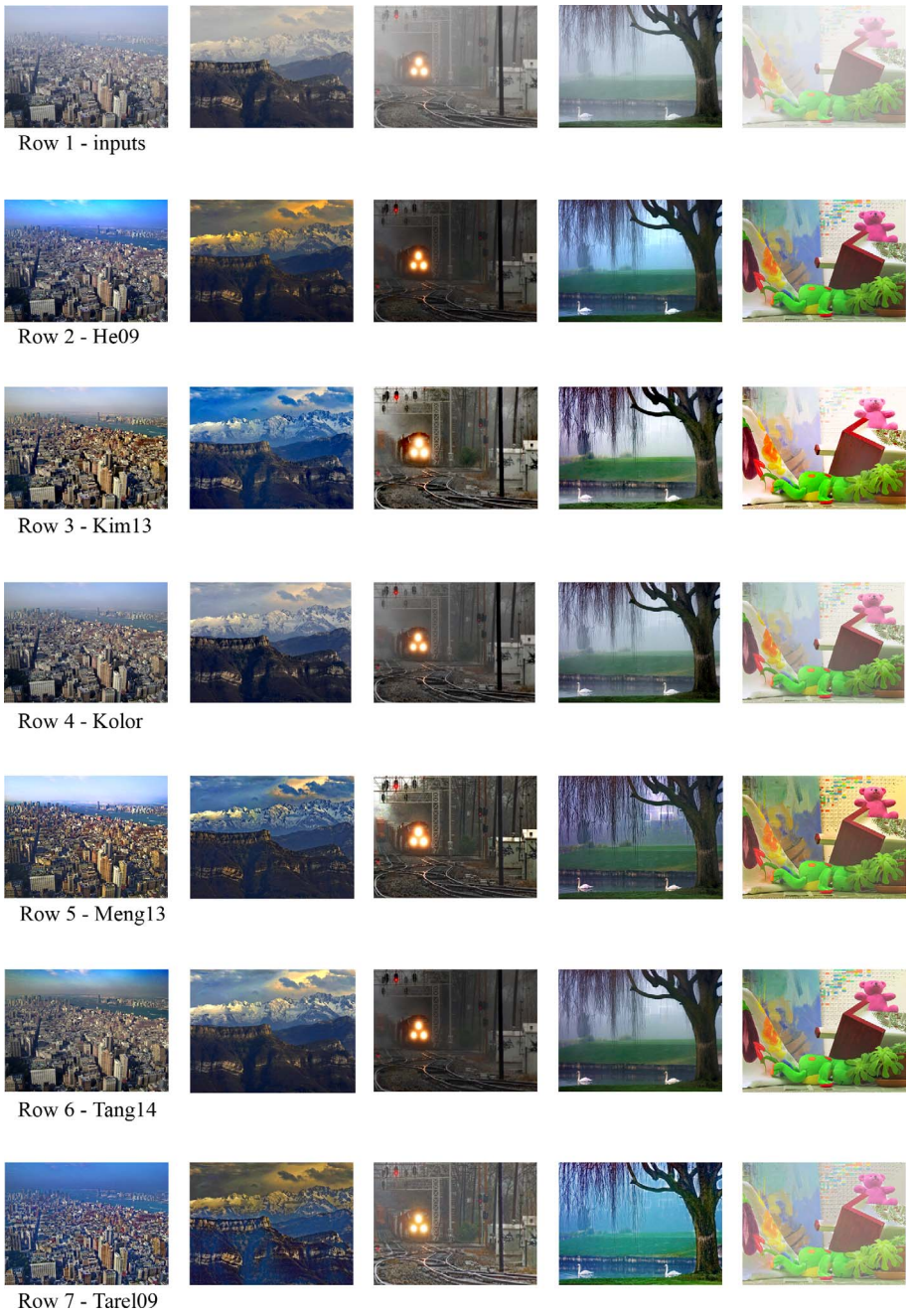

Fig. 6. Output comparison of different dehazing methods – 1.

more appropriate to assess our images. Moreover, VIF(R) shows good correlation with the subjective quality assessment score (MOS) [30]. So VIF(R) is calculated to compare the quality of different dehazing methods. A score closer to 1 indicates a better dehazing method.

4.3. No reference IQA

The unavailability of the reference image in the case of natural outdoor images suggests the use of no reference IQA for the evaluation of dehazed images. Three evaluation descriptors, namely e,$\bar{r}$ and σ are used to compare the quality of the results obtained from other dehazing methods and the proposed method [26]. The value of e is a measure of the ability of the method to restore edges which were invisible in the original image. $\bar{r}$ is the geometric mean of the ratio of the visibility levels. n_s is the number of saturated pixels normalized by the size of the image. For a good quality image, the values of e and $\bar{r}$ should be high and the value of σ should be low.

Standard deviation (SD) is used as a measure of contrast of the image. An image with a larger value of standard deviation exhibits better contrast. We also calculate the perceptual fog density D which denotes the amount of haze in the image [31,32].

5. Analysis of the results

Output images of different dehazing methods are shown in Figs. 6 and 7 for visual comparison. It can be seen that He's method, though provides good dehazing, results in images which are too dark. In Tarel's result, haze is not completely removed. Among the three color spaces, surround filter in RGB gives the best dehazing effect and colors.

Various quality assessment parameters are calculated for the images in IVCDehazedataset and for the outputs of the proposed method for comparison. The blind evaluation descriptors calculated for different methods are compared in Table 1. Large values of e and $\bar{r}$ indicate better dehazing and Tarel's and Xiao's methods score high in these

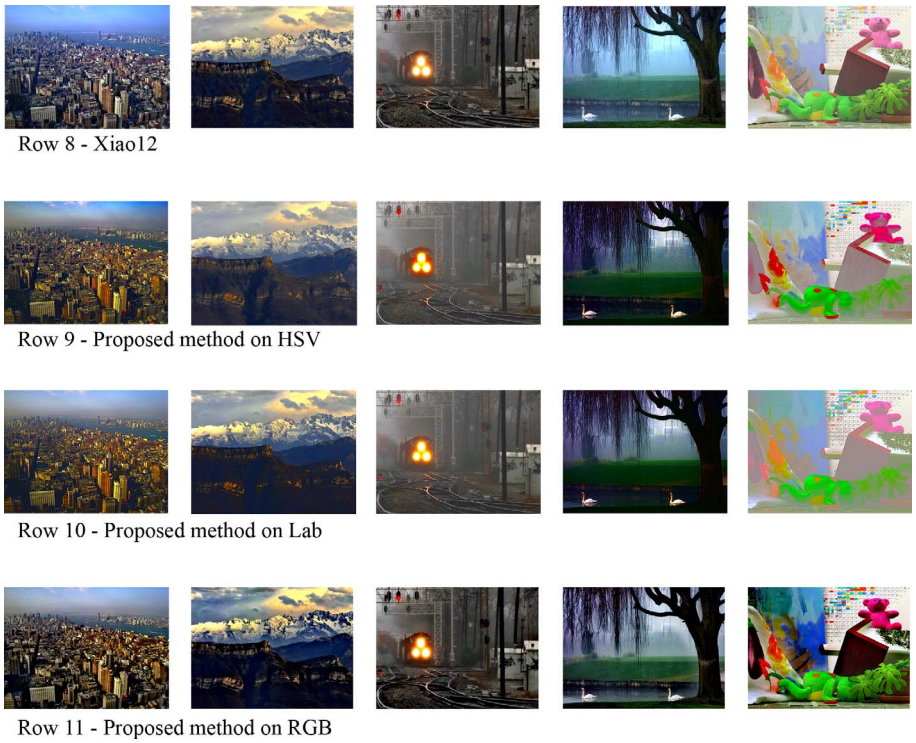

Fig. 7. Output comparison of different dehazing methods – 2.

aspects. It can also be observed that VIF(R) and MOS in their case show good correlation. But there is considerable amount of haze present in their output image as indicated by comparatively large value of D. Surround filter in HSV, Lab and RGB color spaces result in the next highest values of the evaluation descriptors e and $\bar{r}$. Their MOS and VIF (R) values, though not as high as Tarel's and Xiao's methods, exhibit high correlation. Out of all the methods, surround filter on HSV results in the highest standard deviation and surround filter on RGB results in the least amount of haze. Comparing all the methods, Tarel's and Xiao's methods and surround filter on RGB are found to be the most suitable for dehazing.

Comparison of time taken to dehaze three sample images of different sizes, using each method is shown in Table 2. The table shows that our method in RGB, HSV and Lab spaces are faster than the other methods. Complexity of different methods can be compared intuitively in terms of the method used for refining the transmission map. This is also included in Table 2. Since the Gaussian filter in our method automatically smoothens the transmission map, no separate method is used for refining the transmission map. So our method is less complex compared to other methods mentioned above.

Table 2
Complexity comparison of different dehazing methods.

Dehazing	Transmission map refinement method	Execution time for different images		
		Bus 204 × 132	Trees 267 × 188	City 400 × 600
He09	Laplacian matting	2.286	7.540	37.840
Kim13	Guided filter	0.880	1.520	7.120
Meng13	Boundary and contextural constraints	1.498	1.863	13.076
Tarel09	Median of median along lines	0.380	0.702	2.335
Xiao12	Guided joint bilateral filter-linearised	3.490	4.324	11.223
HSV	No separate method	0.273	0.299	1.148
Lab	No separate method	0.597	0.689	2.246
RGB	No separate method	0.443	0.610	2.230

Execution time is in seconds.
bus, trees and city are the sample images.
Size of each sample image in pixels is written below the image name.

6. Conclusion

We propose an effective and computationally simple dehazing method using a simple Gaussian filter which can be implemented in three color spaces. Visual information fidelity in reverse mode and blind evaluation descriptors are calculated for the results of different methods for comparison. Standard deviation and the amount of haze present in the output images of all methods are also compared. The parameters used for evaluation of the results show that our method in RGB color space gives performance comparable to or better than the existing methods. Conventional DCP with Laplacian matting is not suitable for large image dehazing because of its memory requirement. The advantage of the proposed method is that it can be effectively used for large image dehazing also. Its dehazing effects are comparable to the best of the existing methods. The disadvantage here is that the value $c$cannot be chosen arbitrarily. Different input images give appealing results for different values of c. For each image, the optimal value of $c$is selected individually. Good dehazing capability and low computational complexity make this method suitable for real time image dehazing applications.

References

[1] S.G. Narasimhan, S.K. Nayar, Vision and the atmosphere, Int. J. Comput. Vis. 48 (2002) 233–254.
[2] H. Koschmieder, Theorie der horizontalen Sichtweite: Kontrast und Sichtweite, Keim & Nemnich, Frankfurt, 1925.
[3] K. He, J. Sun, X. Tang, Single image haze removal using dark channel prior, IEEE Tran. Pattern Anal. Mach. Intell. 33 (2011) 2341–2353.
[4] R.T. Tan, Visibility in bad weather from a single image, in: IEEE Conf. Computer Vision and Pattern Recognition, Proc. IEEE, 2008, pp. 1–8.
[5] K. He, J. Sun, X. Tang, Guided image filtering, in: IEEE tran. PAMI, Vol. 35 of IEEE, 2013, pp. 1397–1409.
[6] R. Fattal, Single image dehazing, in: J.C. Hart (Ed.), Trans. Graphics (TOG), Vol. 27 of Proc. ACM SIGGRAPH 08, 2008, p. 72.
[7] J.-P. Tarel, N. Hautiere, Fast visibility restoration from a single color or gray level

image, in: 12th Intl. Conf. Computer Vision, Proc. IEEE, 2009, pp. 2201–2208.
[8] Qi, et al., Image dehazing based on structure preserving, Optik-Int. J. Light Electron Opt. 126 (2015) 3400–3406.
[9] Yu, et al., Real-time single image dehazing using block-to-pixel interpolation and adaptive dark channel prior, IET Image Proc. 9 (2015) 725–734.
[10] C. Xiao, J. Gan, Fast image dehazing using guided joint bilateral filter, Vis. Computer. 28 (2012) 713–721.
[11] E.H. Land, Recent advances in retinex theory and some implications for cortical computations: color vision and the natural image, Proc. Natl. Acad. Sci. USA 80 (1983) 5163.
[12] K. Ma, W. Liu, Z. Wang, Perceptual evaluation of single image dehazing algorithms, in: Image Processing, Proc. IEEE, 2015, pp. 3600–3604.
[13] Waterloo ivc dehazed image database, <https://ivc.uwaterloo.ca/>, (Accessed: 2016-12-18).
[14] D.J. Jobson, Z. Rahman, G.A. Woodell, A multiscale retinex for bridging the gap between color images and the human observation of scenes, IEEE Trans. Image Process. 6 (1997) 965–976.
[15] J. Long, Z. Shi, W. Tang, Fast haze removal for a single remote sensing image using dark channel prior, in: Computer Vision in Remote Sensing (CVRS), 2012 International Conference on, IEEE, 2012, pp. 132–135.
[16] H.-G. Lee, S. Yang, J.-Y. Sim, Color preserving contrast enhancement for low light level images based on retinex, in: M.H. Loew (Ed.), 2015 Asia-Pacific Signal and Information Processing Association Annual Summit and Conference (APSIPA), Proc. IEEE, 2015, pp. 884–887.
[17] M.C. Hanumantharaju, M. Ravishankar, D.R. Rameshbabu, Natural color image enhancement based on modified multiscale retinex algorithm and performance evaluation using wavelet energy, in: Recent Advances in Intelligent Informatics, Springer, 2004, pp. 83–89.
[18] J. Wu, Z. Wang, Z. Fang, Application of retinex in color restoration of image enhancement to night image, in: 2nd Intl. Congr. Image and Signal Processing (CISP'09), Proc. IEEE, 2009, pp. 1–4.
[19] Yan, et al., A highly parallel framework for hevc coding unit partitioning tree decision on many-core processors, IEEE Signal Process. Lett. 21 (2014) 573–576.
[20] Yan, et al., Efficient parallel framework for hevc motion estimation on many-core processors, IEEE Trans. Circ. Syst. Video Technol. 24 (2014) 2077–2089.
[21] T. Mertens, J. Kautz, F.V. Reeth, Exposure fusion, in: 15th Pacific Conf. Computer Graphics and Applications, Proc. IEEE, 2007, pp. 382 – 390.
[22] D.M. Chandler, K.H. Lim, S.S. Hemami, Effects of spatial correlations and global precedence on the visual fidelity of distorted images, in: Electronic Imaging 2006, Proc. SPIE, 2006, pp. 60570F–60570F.
[23] Z. Wang, et al., Image quality assessment: from error visibility to structural similarity, IEEE Tran. Image Process. 13 (2004) 600–612.
[24] Z. Wang, et al., Quality-aware images, IEEE Tran. Image Process. 15 (2006) 1680–1689.
[25] P. Ye, D. Doermann, No-reference image quality assessment based on visual codebook, in: Intl. Conf. Image Processing (ICIP), Proc. IEEE, 2011, pp. 3089–3092.
[26] N. Hautiere, et al., Blind contrast enhancement assessment by gradient ratioing at visible edges, Image Anal. Stereol. 27 (2008) 87–95.
[27] C. Ancuti, C. Ancuti, C.D. Vleeschouwer, D-hazy: a dataset to evaluate quantitatively dehazing algorithms, in: IEEE Intl. Conf. ICIP, Proc. IEEE, 2016, pp. 2226–2230.
[28] H.R. Sheikh, A.C. Bovik, Image information and visual quality, IEEE Trans. Image Proc. 15 (2006) 430–444.
[29] H.R. Sheikh, A.C. Bovik, A visual information fidelity approach to video quality assessment, in: The First Intl. Ws. Video Processing and Quality Metrics for Consumer Electronics, Citeseer, 2005, pp. 23–25.
[30] A. Pattem, P. Sankaran, Visual information fidelity in evaluating retinex enhancement algorithms, in: Communication and Signal Processing, in: Proc. IEEE, 2014, pp. 167 – 171.
[31] L.K. Choi, J. You, A.C. Bovik, Referenceless prediction of perceptual fog density and perceptual image defogging, IEEE Trans. Image Proc. 24 (2015) 3888–3901.
[32] Laboratory for image and video engineering, https://live.ece.utexas.edu/research/fogFADE_release.zip, (Accessed: 2016-12-20).